

SERS-activating effect of chlorides on borate-stabilized silver nanoparticles: formation of new reduced adsorption sites and induced nanoparticle fusion

Ivana Šloufová,^{ab} Karolína Šišková,^{†a} Blanka Vlčková^{**a} and Josef Štěpánek^c

Received 23rd November 2007, Accepted 1st February 2008

First published as an Advance Article on the web 3rd March 2008

DOI: 10.1039/b718178g

Changes in morphology, surface reactivity and surface-enhancement of Raman scattering induced by modification of borate-stabilized Ag nanoparticles by adsorbed chlorides have been explored using TEM, EDX analysis and SERS spectra of probing adsorbate 2,2'-bipyridine (bpy) excited at 514.5 nm and evaluated by factor analysis. At fractional coverages of the parent Ag nanoparticles by adsorbed chlorides < 0.6 , the Ag colloid/ Cl^- /bpy systems were found to be constituted by fractal aggregates of Ag nanoparticles fairly uniform in size (10 ± 2 nm) and SERS spectra of Ag^+ -bpy surface species were detected. The latter result was interpreted in terms of the presence of oxidized Ag^+ and/or Ag_n^+ adsorption sites, which have been encountered also in systems with the chemically untreated Ag nanoparticles. At chloride coverages > 0.6 , a fusion of fractal aggregates into the compact aggregates of touching and/or interpenetrating Ag nanoparticles has been observed and found to be accompanied by the formation of another surface species, Ag-bpy, as well as by the increase of the overall SERS enhancement of bpy by factor of 40. The same Ag-bpy surface species has been detected under the strongly reducing conditions of reduction of silver nitrate by sodium borohydride in the presence of bpy. The formation of Ag-bpy is thus interpreted in terms of the stabilization of reduced Ag(0) adsorption sites by adsorbed bpy. The formation of reduced adsorption sites on Ag nanoparticle surfaces at chloride coverages > 0.6 is discussed in terms of local changes in the work function of Ag. Finally, the SERS spectral detection of Ag-bpy species is proposed as a tool for probing the presence of reduced Ag(0) adsorption sites in systems with chemically modified Ag nanoparticles.

1. Introduction

The phenomenon of SERS (surface-enhanced Raman scattering) originates from a simultaneous interaction of light with free-electron-like metal (*e.g.* Ag) nanostructures and molecular species located at their surfaces. In the case of molecules adsorbed on Ag nanoparticle surfaces, both the incident and the Raman scattered light are enhanced *via* resonance Mie scattering by the Ag nanoparticle assembly. This process is dubbed the electromagnetic (EM) mechanism of SERS. Provided that the incident light obeys simultaneously the Mie resonance condition and the molecular resonance condition for a particular surface species (which can be either an only weakly perturbed molecule and/or a surface complex), molecular resonance mechanism (usually dubbed the chemical mechanism of SERS for surface complexes) contributes to the overall SERS enhancement.¹

In the last decade, SERS became a subject of reinforced interest due to a possibility of achieving a single molecule detection level.^{2–7} SERS-activation of Ag nanoparticles by chlorides appears to play an important role in single molecule SERS, since it has been employed in the majority of the published studies for the activation of Ag colloids stabilized by adsorbed citrate.^{2–7} For example, Brus and coworkers observed a direct relationship between the chloride concentration and the SERS signal increase in system with Ag nanoparticles and rhodamine 6G.⁴ In a seminal earlier study, Hildebrandt and Stockburger attributed the SERS activating effect of chlorides in this particular system to the formation of new, specific adsorption sites.⁸ Weitz and coworkers reported formation of reduced Au(0) adsorption sites by chloride-modification of citrate-stabilized Au nanoparticles.⁹ SERS-activation by chlorides was encountered in systems with Ag nanoparticles prepared by reduction of silver nitrate by sodium borohydride (bh-red Ag colloid, stabilized by adsorbed borates) as well,^{10–12} and the adsorbate specificity of such activation has been pointed out. In summation, regardless the type of Ag nanoparticle stabilization, the SERS-activation by chlorides was usually related to the chemical mechanism of SERS. Specifically, the formation of Ag-2,2-bipyridine (Ag-bpy) surface species exhibiting a photoinduced charge transfer at ~ 540 nm (and hence a chemical mechanism contribution to SERS at excitations close to this wavelength) was reported to

^a Department of Physical and Macromolecular Chemistry, Charles University, Hlavova 2030, Prague 2, 12840, Czech Republic. E-mail: vlč@natur.cuni.cz

^b Institute of Macromolecular Chemistry, AS CR, Heyrovský sq. 2, Prague 6, 16206, Czech Republic

^c Institute of Physics, Charles University, Ke Karlovu 5, Prague 2, 12116, Czech Republic

[†] Present address: Institute of Macromolecular Chemistry, AS CR, Heyrovský sq. 2, Prague 6, 16206, Czech Republic.

result from the treatment of bh-Ag colloid by high HCl concentrations.¹² The identification of the Ag-bpy surface species as distinctly different from Ag⁺-bpy surface species encountered on Ag nanoparticle surfaces in the absence of and/or at low HCl concentrations (and exhibiting no CT transition) pointed towards a possibility that, at higher HCl concentrations, new adsorption sites are formed on Ag nanoparticle surface and are stabilized by adsorption of bpy.¹²

Nevertheless, chloride-induced changes in Ag nanoparticle morphology and surface plasmon extinction (SPE) spectra (for both citrate and borate stabilized Ag nanoparticle hydrosols) have been reported and successfully employed in NIR-SERS (FT-SERS excited by 1064 nm wavelength) owing to the extension of SPE of Ag hydrosols into this spectral region after the chloride treatment (particularly in acidic ambient).^{12–15}

It should be noted that a possible contribution of the EM mechanism to the chloride-activation (*i.e.* the overall SERS signal increase induced by addition of chlorides) *via* chloride-induced changes of the morphology of Ag nanoparticles and/or of their assembly, as well as the chemical mechanism contribution *via* molecular resonance with a CT transition of a newly formed surface complex will be dependent on the wavelength of radiation selected for the excitation of SERS. Both the magnitude and the mechanism of chloride activation may thus vary substantially with the excitation wavelength selected for a particular SERS experiment.

In this paper, we contribute to the subject first by a series of experiments in which both the formation of new adsorption sites and the morphology changes in systems with bh-red. Ag nanoparticles have been encountered and are followed as a function of chloride concentration in both acidic and neutral media. The formation of new adsorption sites is monitored by the SERS spectral detection of the Ag-bpy surface species (which was shown earlier¹² to exhibit a photoinduced CT, and has been unequivocally characterized spectrally by factor analysis in this paper). Morphology changes are followed by TEM imaging of deposited Ag colloid/Cl⁻/bpy systems and/or monolayer nanoparticulate films prepared from them, and manifest themselves by the fusion of Ag nanoparticles into small aggregates of touching and/or interpenetrating particles. The experiments reveal that both the above-mentioned processes progress only at and above a certain threshold concentration of chlorides in the system which corresponds to *ca.* 0.6 monolayer coverage of Ag nanoparticles by adsorbed chlorides (as estimated from the results of EDX analysis). SERS-activation by a factor of 40 at 514.5 nm excitation was determined to result from the incubation of Ag colloid/bpy systems by chloride concentrations above the threshold value.

Furthermore, we report experiments targeted on the characterization of new adsorption sites identified on chloride modified Ag nanoparticles. In particular, we provide evidence that the same adsorption sites are formed under the strongly reducing conditions of Ag nanoparticle growth driven by reduction of silver nitrate by sodium borohydride, and are stabilized by bpy forming the Ag-bpy surface species. In the light of these results, we rise arguments in favor of the reduced Ag(0) character of the adsorption sites generated by high surface concentrations of chlorides adsorbed on Ag nanoparticles.

2. Experimental

Materials: Analytical grade chemicals and distilled deionized or doubly distilled deionized water were used for all sample preparations: NaBH₄ (Merck), AgNO₃ (Aldrich), 2,2'-bipyridine (Merck), EtOH (Merck, UVASOL), HCl (Lachema), NaCl (Lachema).

Preparation procedures: *Ag colloid (Ag nanoparticle hydrosol)* was prepared by reduction of silver nitrate by sodium borohydride according to the procedure II described in ref. 16.

Ag colloid/bpy/HCl systems were prepared by adding 20 μ L of a 1×10^{-2} M aqueous solution of bpy and 10 μ L of 1×10^{-2} M aqueous HCl to 2 mL of Ag colloid. Final HCl concentration in the systems varied from 5.0×10^{-5} M to 6.7×10^{-3} M. These systems were used as samples for the set of SERS spectra subjected to factor analysis (FA). For SERS spectral intensity measurements, ethanol (240 μ L) was introduced into the systems as internal intensity standard.

Ag colloid/bpy/NaCl systems were prepared analogously to the *Ag colloid/bpy/HCl* systems with final NaCl concentrations ranging from 5.0×10^{-5} to 1.1×10^{-1} M. The systems for determination of the SERS spectral detection limits of (a) Ag⁺-bpy and (b) Ag-bpy species were constituted by 2 mL of Ag colloid, 10 μ L of (a) 1×10^{-2} M HCl, or (b) 1 M HCl respectively, and 10 μ L of $c_x[M]$ bpy solution which varied from 1×10^{-2} to 1×10^{-8} M. The overall bpy concentrations in the systems were in the 5×10^{-5} – 5×10^{-11} M range.

Monolayer nanoparticulate *Ag colloid/HCl-bpy* and/or *Ag colloid/NaCl-bpy* films for TEM and EDX studies were prepared in a water-dichloromethane system according to the procedure described, in general, in ref. 17. Briefly, to 2 mL of Ag colloid, 10 μ L of 1 M HCl and/or 1 M NaCl were added, mixed with 2 mL of 2×10^{-3} M bpy in CH₂Cl₂ and vigorously shaken up for several minutes until formation of a distinct nanoparticulate film at the interface between the two liquids was observable. The re-assembling of the multilayer nanoparticulate film into a monolayer one was accomplished by the procedure described in ref. 18.

Systems in which Ag nanoparticles were grown by the reduction of silver nitrate by sodium borohydride in the presence of bpy (denoted *bpy-Ag colloid*) were prepared as follows: 1.1×10^{-3} M aqueous solution of NaBH₄ prepared by dissolving 3.5 mg of NaBH₄ in 75 mL of doubly distilled, deionized water was cooled to 2 °C in an ice-bath. To this solution, 80 μ L aliquots of aqueous solution of bpy of the appropriate concentration to yield 1×10^{-5} M and/or 1×10^{-6} M overall concentration of bpy in system were added. After *ca.* 2 min of stirring (with a magnetic stirrer at a constant speed), 4.5 mL of 4.4×10^{-3} M solution of AgNO₃ (prepared by dissolving 13.52 mg of AgNO₃ in 18 mL of doubly distilled, deionized water and precooled to *ca.* 8 °C), were added dropwise (1 drop/3 s) at constant stirring. Stirring was continued without interruption for another 45 min.

Instrumentation

SERS spectra were recorded at room temperature using a multichannel Raman spectrometer equipped with a Monospec-600 monochromator and a liquid N₂-cooled CCD detector system (Princeton Instruments). A holographic notch-plus

filter (Kaiser) was placed in front of the entrance slit of the monochromator to remove the Rayleigh line from scattered light. The Raman scattering was collected in a right-angle scattering geometry. Excitation was provided with the 514.5 nm line of an argon ion laser ILA-120 (Carl-Zeiss, Jena). The average laser power at the sample in a 10 mm quartz glass five-window cuvette was about 88 mW. Spectra were accumulated for 60 s. Basic spectral data treatment was employed¹⁹ and, in selected cases, included baseline correction. Smoothing of the spectra was avoided.

Transmission electron microscopy (TEM) imaging of the Ag nanoparticle systems and films deposited on carbon-coated Cu grids was performed with a JEOL-JEM 200 CX transmission electron microscope.

EDX analysis was accomplished with a JEOL SUPERPROBE 733 scanning electron microscope equipped with JXA 733 X-ray analyzer and KEVEX Δ EDX spectrometer using monolayer Ag nanoparticulate films deposited on carbon blocks of 5 mm in diameter and of a several mm height as samples.

Factor analysis of SERRS spectra

The sets of SERS spectra measured from *Ag colloid/bpy/HCl* systems as a function of increasing HCl concentration were treated by factor analysis (FA) procedure,²⁰ using a singular value decomposition algorithm.^{21,22} The procedure provides a set of orthonormal subspectra $S_j(\nu)$, singular values W_j representing the statistical weight of each of the subspectrum, and a square matrix of virial coefficients V_{ij} , which are related to the experimental spectra $Y_i(\nu)$ by eqn (1):

$$Y_i(\nu) = \sum_{j=1}^N W_j V_{ij} S_j(\nu) \quad i, j = 1, 2, \dots, N, \quad (1)$$

where N is the number of the experimental spectra.

The original dimension of the data set N is then reduced to a factor dimension $M < N$ by finding the minimal value of M for which difference between the right and the left hand side of the eqn (2) will be within the experimental error.

$$Y_i(\nu) \approx \sum_{j=1}^M W_j V_{ij} S_j(\nu) \quad i = 1, 2, \dots, N; \quad j = 1, 2, \dots, M \quad (2)$$

The value of the factor dimension M can be determined from the plot of the singular values as a function of the subspectrum number, and corresponds to the number of independent spectral components which can be resolved in the analyzed spectral set. The spectra of the pure spectral components (forms) P_n ($n = 1, 2, \dots, M$) can be obtained as a linear combination of the statistically relevant subspectra S_j :

$$P_n(\nu) = \sum_{j=1}^M c_{nj} S_j(\nu) \quad n = 1, 2, \dots, M; \quad j = 1, 2, \dots, M \quad (3)$$

The procedure by which the spectra of the pure spectral components were obtained has been described in detail in ref. 21.

3. Results and discussion

3.1 SERS spectra and morphology of systems constituted by chloride-modified Ag nanoparticles and bpy

3.1.1 SERS spectra and TEM images of the Ag colloid/bpy/HCl system as a function of HCl concentration. A set of 12 SERS spectra of the Ag colloid/bpy (1×10^{-4} M)/HCl system measured as a function of HCl concentration in the 4.4×10^{-5} to 6.7×10^{-3} M range at the 514.5 nm excitation wavelength was subjected to FA. The plot of the singular values W versus the subspectrum number (S_1 – S_{12}) (Fig. 1A) indicates that only the first two subspectra S_1 and S_2 (shown in Fig. 1B) significantly contribute to the overall experimental spectral set, and hence the factor dimension M of the problem is two. Using eqn (2) and the determined value of $M = 2$ (i.e. $j = 1, 2$), all the experimental spectra $Y_i(\nu)$ ($i = 1 \dots 12$) were fully reconstructed. The $M = 2$ value indicates that only

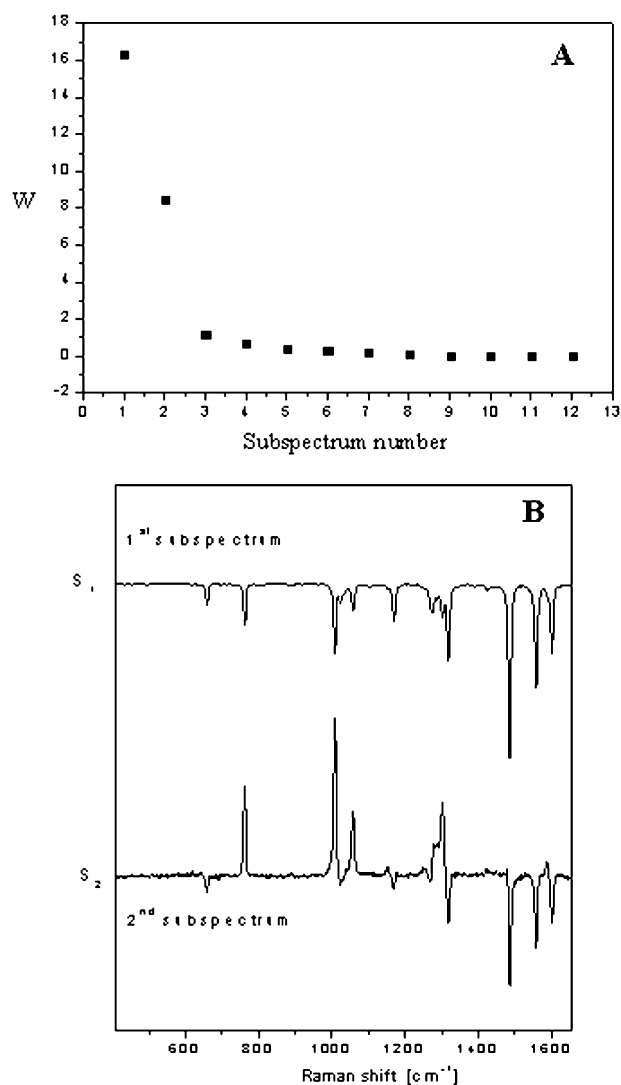


Fig. 1 Results of FA (factor analysis): (A) Singular numbers W vs. subspectrum number; (B) 1st and 2nd subspectrum. The 1st subspectrum reflects principal spectral features of the overall spectral set, the 2nd subspectrum features major differences between the spectra within the set.

two spectrally different species (pure components) contribute to all the experimental spectra within the analysed set.

The SERS spectra of these two pure spectral forms obtained as proper linear combinations of the first two subspectra are shown in Fig. 2. The SERS spectrum of the pure spectral component in Fig. 2A is consistent with the SERS spectra of form I of adsorbed bpy in ref. 11 and 12 which, due to its perfect spectral match with the synthetically prepared complex unit $[\text{Ag}(\text{bpy}_2)]^+$,^{11,12,23} is attributed to $\text{Ag}^+\text{-bpy}$ (or $\text{Ag}_n^+\text{-bpy}$) surface species. The SERS spectrum of the second pure spectral component (Fig. 2B) matches those of form III Ag-bpy surface species (at 514.5 nm excitation).^{11,12} FA thus provides us with a proof that there are only the two above mentioned spectral forms of adsorbed bpy in systems with Ag nanoparticles and HCl throughout the overall range of HCl concentrations, as well as with the unambiguous assignment of the SERS spectral bands to one or the other surface species.

The detailed assignment of SERS spectral bands of $\text{Ag}^+\text{-bpy}$ and of Ag-bpy (form III) surface species has been reported in ref. 12. The assignment has shown that in both surface species, bpy is bidentately coordinated to the Ag^+ and/or $\text{Ag}(0)$ active sites adopting thus a *cis*-conformation. Nevertheless, the differences in SERS spectral patterns between $\text{Ag}^+\text{-bpy}$ and Ag-bpy (form III) (in particular, the shift of the wavenumber of the bpy breathing mode from 1010 cm^{-1} in $\text{Ag}^+\text{-bpy}$ to 1024 cm^{-1} in Ag-bpy SERS spectra) indicate a stronger bonding interaction between bpy and the $\text{Ag}(0)$ active site than between bpy and Ag^+ .¹² Additionally, the differences in the SERS spectral patterns are accompanied by differences in the electronic structure of the two surface species, namely the existence of a photoinduced CT transition at 540 nm in the case of Ag-bpy, and its absence in $\text{Ag}^+\text{-bpy}$.

Furthermore, since the 514.5 nm wavelength used for the excitation of the SERS spectral set analysed by FA falls into the contour of the photoinduced CT band with maximum at $\sim 540\text{ nm}$ (ref. 12), Ag-bpy (form III) surface species experiences a CT resonance (chemical mechanism) contribution to the overall SERS signal at this particular excitation wave-

length. Owing to this near-resonance condition, the results of FA, in particular the fact that the third subspectrum consists only of noise fluctuations, also indicate that there is no substantial shift (*i.e.* a wavelength change) of the photoinduced CT transition band of Ag-bpy with the increasing HCl concentration in the system. It can be anticipated that should such a shift occur, it would cause the changes of the relative intensities of Ag-bpy spectral bands with the increasing HCl concentration (similar to those observed in SERS spectra with the change of excitation wavelength in ref. 12). These changes would be revealed by FA through obtaining a third subspectrum with a meaningful signal and a higher statistical weight.

The relative intensities of the normalized bands of each form were obtained from the SERS spectral set of Ag colloid/bpy ($1 \times 10^{-4}\text{ M}$)/HCl systems containing ethanol as internal intensity standard, and were plotted as a function of HCl concentration in the system. Examples of such plots for the 1303 cm^{-1} band of $\text{Ag}^+\text{-bpy}$ (curve a) and the 1318 cm^{-1} band of Ag-bpy (curve b) are shown in Fig. 3. The plot (curve b) of the Ag-bpy band shows that this spectral band becomes detectable at a threshold HCl concentration of $5 \times 10^{-4}\text{ M}$. At HCl concentrations increasing above this value, the normalized relative intensity of this band increases, and reaches saturation at $3.5 \times 10^{-3}\text{ M}$ HCl concentration in the system. Analogous sigmoidally shaped plots with the same threshold and saturation HCl concentrations were obtained for all other spectral bands of Ag-bpy. In contrast, the normalized relative intensities of the 1303 cm^{-1} band of $\text{Ag}^+\text{-bpy}$ (curve a) (and all other bands of this species) remain virtually constant throughout the overall HCl concentration range. In summation, the plots in Fig. 3 demonstrate that in systems with HCl concentrations below the threshold value, only $\text{Ag}^+\text{-bpy}$ is detected, while for HCl concentrations above the threshold value, SERS spectra provide evidence of coexistence of both surface species. These results indicate that Ag^+ adsorption sites stabilized by bpy remain most probably fully or partially intact with the HCl concentration increasing above the

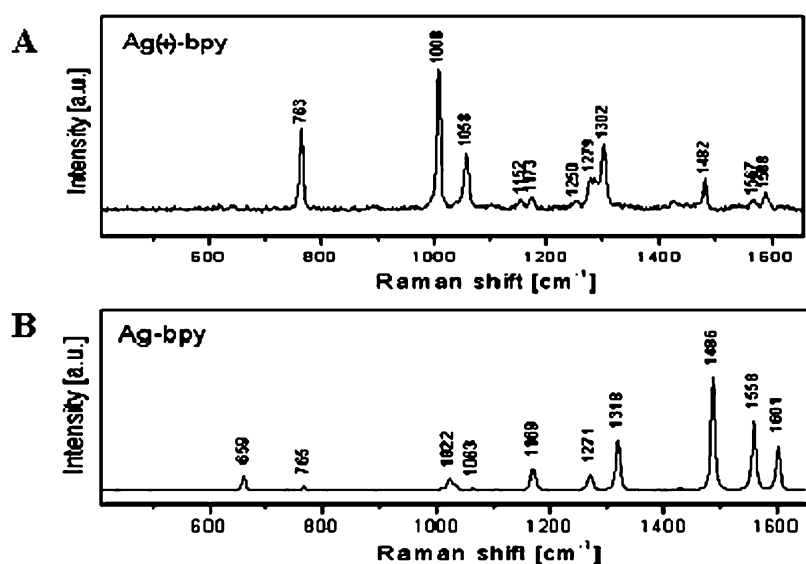


Fig. 2 Pure spectral components: (A) $\text{Ag}^+\text{-bpy}$ and (B) Ag-bpy surface species.

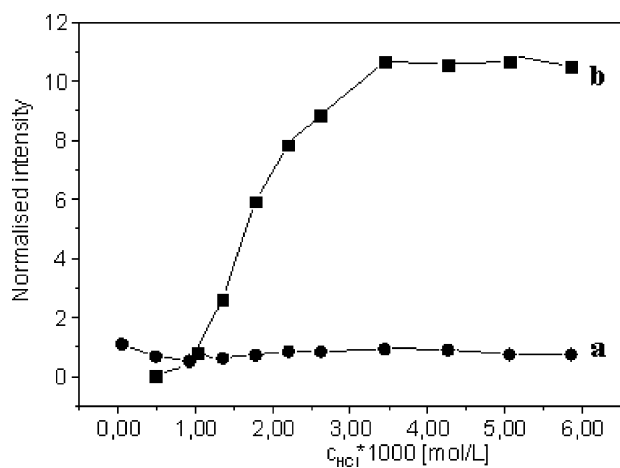


Fig. 3 Normalised intensities of the selected bands of the bpy surface species plotted as a function of HCl concentration: (a) the 1303 cm^{-1} band of the Ag^+ -bpy surface species and (b) the 1318 cm^{-1} band of the Ag-bpy surface species.

threshold concentration, while new adsorption sites are formed and stabilized by bpy forming Ag-bpy surface species.

The principal changes in morphologies of Ag nanoparticle assemblies deposited from Ag colloid/HCl bpy systems with HCl concentration increasing in the 5×10^{-5} – 5×10^{-3} M range were revealed by TEM imaging at two different magnifications (Fig. 4). The TEM images of the system with 5×10^{-5} M HCl in Fig. 4A depict a typical fractal aggregate^{9,24} of Ag nanoparticles with a rather narrow size distribution and mean size of 10 ± 2 nm. With the increasing HCl concentration (Fig. 4B–D), Ag nanoparticles in these aggregates fuse together forming substantially more compact aggregates of nanoparticles enlarged in size to 40–100 nm. Nevertheless, there are indications at higher magnifications that a substantial fraction of these large objects can be aggregates of touching and/or even interpenetrating (*e.g.* twinned) particles. Importantly, some Ag nanoparticles fused into compact aggregates are already observable in Fig. 4B, *i.e.* on the TEM image of the Ag colloid/bpy/HCl system with the 5×10^{-4} M HCl, which is

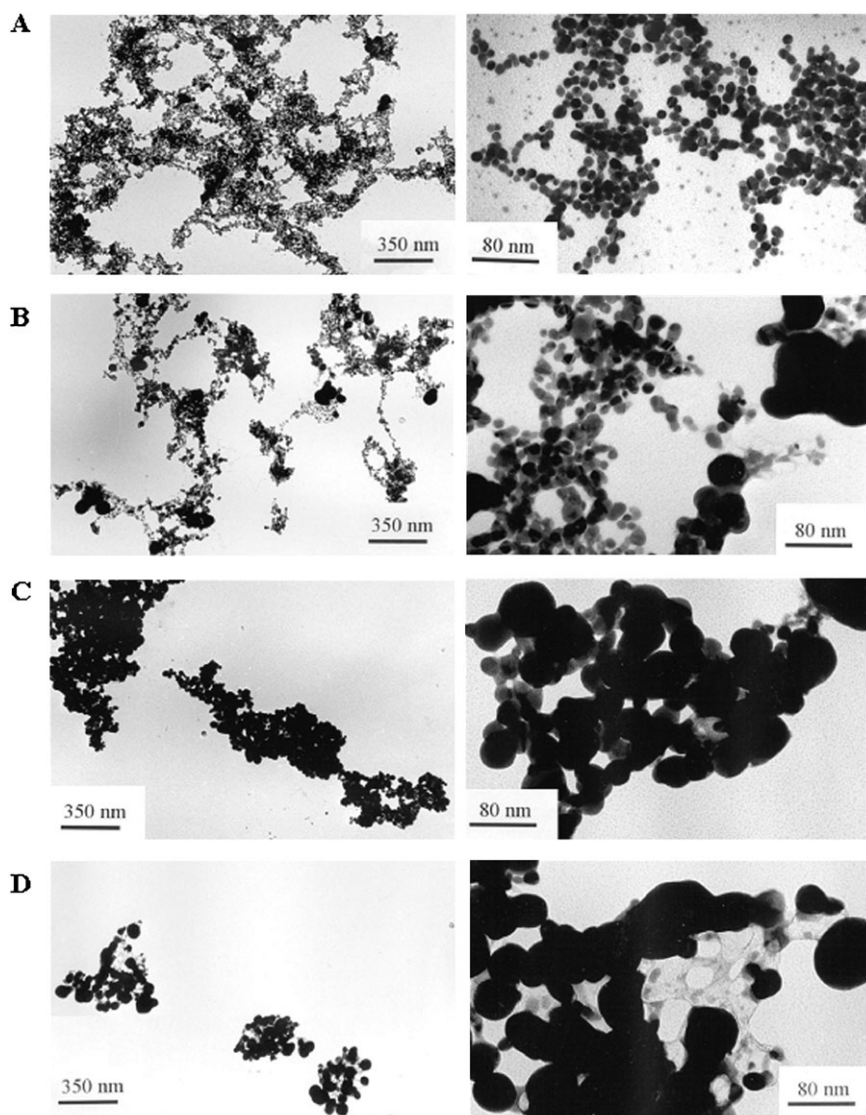


Fig. 4 TEM images of deposited Ag colloid/bpy/HCl systems with HCl concentrations: (A) 5×10^{-5} M, (B) 5×10^{-4} M, (C) 2.5×10^{-3} M, (D) 5×10^{-3} M.

the threshold concentration for the Ag-bpy surface species formation. With the increase of HCl concentration in the systems above the threshold value, both the extent of the morphological changes and the SERS signal intensity of Ag-bpy increase (Fig. 3 and 4). There is thus a possibility that the fusion of Ag nanoparticles into compact aggregates and the formation of new adsorption sites may be mutually related, and conditioned by a particular threshold HCl concentration. It should also be noted that aggregate morphologies similar to those in Fig. 4D were reported earlier by Garcia-Ramos for the HCl-modified systems of Ag nanoparticles with other adsorbates.¹⁵ As a next step, we replaced HCl by NaCl to establish whether or not the chloride-induced changes described above manifest themselves also in neutral aqueous ambient (section 3.1.2). Furthermore, since the TEM images of the collapsed 3-D aggregates in Fig. 4 did not allow for visualization of the full details of the induced morphology changes, we prepared and imaged two-dimensional films of Ag nanoparticles treated by chlorides and bpy in both acidic and neutral ambient (section 3.1.3).

3.1.2 Effect of pH on SERS spectra of Ag colloid/bpy/Cl⁻ systems. In Ag colloid/bpy/HCl systems, a step-wise increase of the HCl concentration causes an increase of the Cl⁻ as well as H⁺ concentration, together with the overall ionic strength of the Ag hydrosol. To separate the effect of the decreasing pH from the effect of the increasing chloride concentration and the increasing ionic strength, we investigated SERS spectra of bpy in the Ag colloid/bpy/NaCl system as a function of NaCl concentration. Analysis of the SERS spectra obtained (not shown here) reveals the appearance of the SERS spectral bands of Ag-bpy at NaCl concentrations *ca.* 5×10^{-3} M and higher. We thus provide SERS spectral evidence that Ag-bpy species can be generated by chlorides also in neutral ambient, and that protonation of bpy to H⁺ bpy is not a necessary condition of Ag-bpy formation. On the other hand, it should be noted that the 5×10^{-3} M NaCl threshold concentration for Ag-bpy SERS signal appearance in the Ag colloid/bpy/NaCl system is about one order of magnitude higher than that in the Ag colloid/bpy/HCl system. To explain this difference, the threshold concentrations of HCl and/or NaCl had to be related to actual average surface concentration of chlorides in the particular Ag nanoparticle assemblies. This task was accomplished with help of EDX analysis of 2-D Ag colloid/HCl-bpy and Ag colloid/NaCl-bpy films in the following section 3.1.3.

3.1.3 TEM images and EDX analysis of deposited 2-D Ag colloid/HCl-bpy and Ag colloid/NaCl-bpy films. The TEM images of 2-D Ag colloid-bpy, Ag colloid/NaCl-bpy and Ag colloid/HCl-bpy films are compared in Fig. 5. Equal, 5×10^{-3} M concentrations of HCl and/or NaCl were used for the treatment of the Ag nanoparticles in aqueous phase in the course of the film preparations. This concentration represents the NaCl threshold concentration for both the Ag-bpy surface species formation (section 3.1.2) and for the onset of the morphology changes within the 2-D Ag nanoparticle assembly (Fig. 5B). In the case of HCl, this concentration is one order of magnitude above the threshold concentration and very close

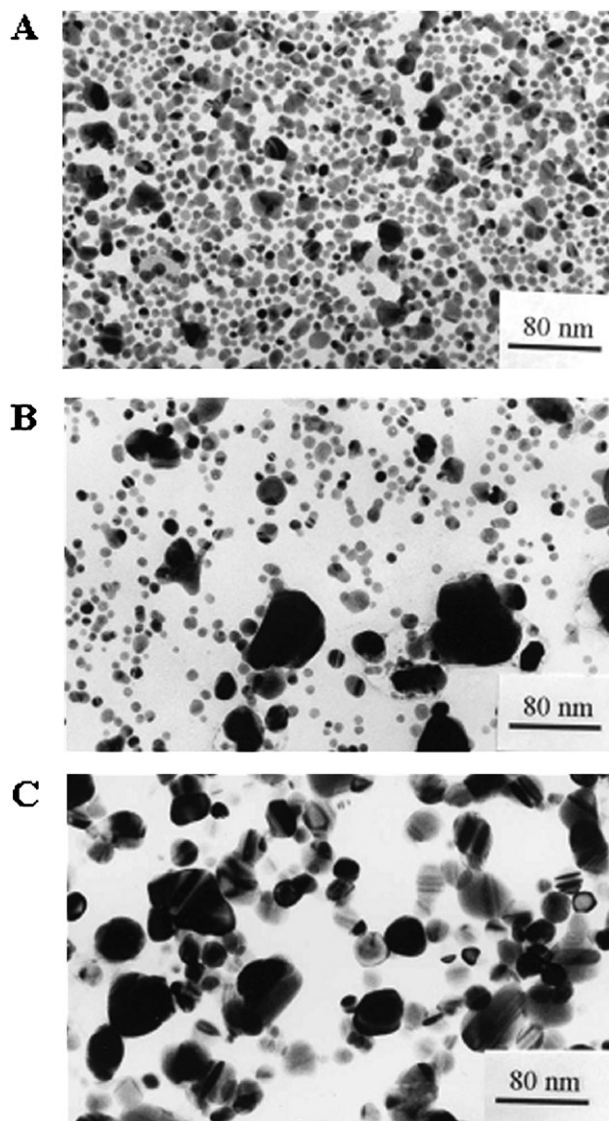


Fig. 5 TEM images of 2-D assemblies: (A) Ag colloid-bpy, (B) Ag colloid/NaCl-bpy and (C) Ag colloid/HCl-bpy films.

to the saturation concentration of HCl required for Ag-bpy formation (section 3.1.1).

The comparison of Fig. 5B and C reveals a substantially larger extent of Ag nanoparticle morphology changes for the Ag colloid/HCl-bpy than for Ag colloid/NaCl-bpy film. Furthermore, the Ag:Cl molar ratios obtained by multiparticle EDX analysis are 1 : 0.12 and 1 : 0.17 for Ag colloid/NaCl-bpy (Fig. 5B) and Ag colloid/HCl-bpy (Fig. 5C) films, respectively. The higher fraction of adsorbed chlorides detected in the film of Ag nanoparticles treated by HCl in comparison to that treated by the same concentration of NaCl indicates promotion of chloride adsorption in acidic media. An analogous effect of pH on adsorption of halides on Ag electrode surfaces was revealed by a XPS study.²⁵ The fractional coverage of Ag nanoparticles by chlorides at the NaCl threshold concentration is roughly estimated to 0.6 monolayer (details in ref. 26). The amount of chlorides in Ag colloid/HCl-bpy film corresponds to 0.8–0.9 fractional coverage of Ag nanoparticles,

however, this very rough estimate is further biased by the large morphology changes undergone by this system.

TEM images at high magnifications (Fig. 6) show the details of typical Ag nanoparticles and their compact aggregate morphologies encountered in Fig. 5C, in particular a compact aggregate of three particles, in which the parent Ag nanoparticles constituting the aggregate can be identified by three different directions of diffraction fringes (Fig. 6A), and touching Ag nanoparticles (Fig. 6B). Model morphologies analogous to those found experimentally in the TEM images of Ag nanoparticle assemblies modified by chlorides at fractional coverages >0.6 (Fig. 4B–D, 5B, C and 6), namely the dimers of touching and interpenetrating particles and the chains of fused particles, were the subjects of theoretical treatments.^{27–29} By these calculations, substantial SERS enhancements by the EM mechanism of SERS are predicted to be experienced by molecules placed in specific locations of such morphologies, in particular in interstices between particles. The formation of such morphologies thus appears to be of importance for SERS spectral studies.

3.1.4 Activating effect of chlorides on SERS of bpy at 514.5 nm excitation. The SERS spectra of Ag colloid/HCl/bpy systems as a function of HCl concentration were measured for bpy concentrations varied in the 1×10^{-4} – 1×10^{-8} M range and interpreted with help of the Ag^+ -bpy and Ag-bpy species SERS spectra obtained by FA (section 3.1.1, Fig. 2). The HCl threshold concentration of Ag-bpy signal appearance was found to be independent on the concentration of bpy in the system (repeatedly achieving the 5×10^{-4} M HCl value corresponding to 0.6 fractional coverage of parent Ag nanoparticles by adsorbed chlorides). In systems with HCl concentration below this threshold (from now on denoted as S1), Ag^+ -bpy is the only species detected, while at and above this threshold (*i.e.* in systems from now on denoted S2), the major

contribution to the SERS signal is that of Ag-bpy. The concentration values of SERS spectral detection limit of bpy in both types of systems (S1 and S2) were determined at 514.5 nm excitation, using observation of three characteristic bands of the particular surface species in its SERS spectrum as a criterion of its positive detection. Ag^+ -bpy species in the S1 system was still detected at 2×10^{-8} M bpy concentration, while Ag-bpy in S2 was detected at bpy concentration as low as 5×10^{-10} M. Therefore, the transformation of S1 into S2 by increasing the fractional chloride coverage of Ag nanoparticles to and above 0.6 results into an increase of the average enhancement of SERS of bpy at 514.5 nm excitation by a factor of *ca.* 40.

The S1 and S2 Ag colloid/ Cl^- /bpy SERS active systems mutually differ both in the structure of the detected surface species (Ag^+ -bpy in S1 and Ag-bpy in S2) and in the morphology of Ag nanoparticle assembly (S1 in Fig. 4A and S2 in Fig. 4C). The differences originate from an increase of fractional coverage of Ag nanoparticles by adsorbed chlorides above the 0.6 value. We will now attempt to examine how these differences contribute to the about 40 times increase of the overall SERS enhancement in S2 with respect to that in S1 determined experimentally. This increase involves contributions from both the EM mechanism (which is the major enhancement mechanism in both systems) and from the chemical mechanism (which operates only in S2 system).

In particular, SERS excitation profiles reported in ref. 12 indicate that at 514.5 nm excitation there is no chemical mechanism contribution to SERS of Ag^+ -bpy in S1 (hence the EM mechanism is the only mechanism responsible for the overall SERS enhancement estimated to be at least six orders of magnitude), while for Ag-bpy in S2, the EM mechanism enhancement is accompanied by the chemical mechanism enhancement (originating from a CT resonance), the additional contribution of which is about one order of magnitude at 514.5 nm, as estimated from the excitation profiles.¹² Therefore, while the EM mechanism is the major enhancement mechanism in both systems, the difference in the magnitude of the EM mechanism enhancement between S1 and S2 (evaluated at 514.5 nm) can be estimated to only about one order of magnitude, and encompasses the differences in the systems morphologies, and, consequently, in their surface plasmon resonances at 514.5 nm. This relatively small difference can possibly originate from the presence of “hot spots” (strong nanoscale-localized optical fields) in both systems, namely in the fractal aggregates encountered in S1 (Fig. 4A) and in compact aggregates observed in S2 (Fig. 4C). The presence of “hot spots” in fractal Ag nanoparticle aggregates has been both theoretically predicted³⁰ and experimentally proved.³¹ Existence of “hot spots” in compact aggregates of touching and/or interpenetrating (*e.g.* twinned) Ag nanoparticles is anticipated on the basis of theoretical calculations for analogous model morphologies.^{27–29} This explanation appears to be further supported by evaluation of the effect of chlorides on the EM mechanism of SERS based on a comparison of systems with and without “hot spots”.³² In that particular study, a nearly three orders of magnitude higher SERS enhancement by EM mechanism was encountered by the same surface species (at 514.5 nm excitation) in a system with “hot

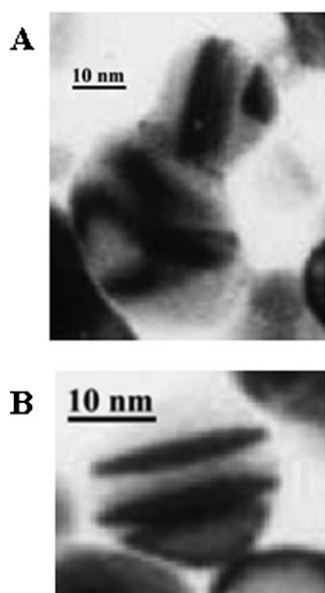


Fig. 6 Details of morphologies of Ag nanoparticles and their aggregates in systems with adsorbed chlorides at fractional coverages above 0.6.

spots" (constituted by compact aggregates of chloride-modified Ag nanoparticles analogous to those observed in S2) than in a system without "hot spots" (containing mostly isolated, unmodified Ag nanoparticles).³²

3.1.5 New adsorption sites on surfaces of chloride-modified Ag nanoparticles. In the further progress of this paper, we focus on the elucidation of the nature of the new adsorption sites formed on Ag nanoparticle surfaces at fractional chloride coverages above *ca.* 0.6, *i.e.* in the S2 systems. A simple calculation of the ratio of bpy molecules and chloride anions at the limit of SERS spectral detection of Ag-bpy has shown that for 6×10^{11} adsorbed bpy molecules (assuming a complete adsorption of bpy from the 5×10^{-10} M solution), 3×10^{16} adsorbed chloride ions are required for Ag-bpy species formation, which corresponds to about 4–5 orders of magnitude excess of chlorides over bpy molecules (details in ref. 26). Therefore, we consider the original explanation of Ag-bpy (form III) structure as a single bpy molecule co-adsorbed with a single chloride anion on a Ag^+ adsorption site reported in ref. 11 as highly improbable, since it is not compatible with the large excess of chlorides over bpy molecules required for its formation. A more probable explanation is that the threshold coverage of Ag nanoparticles is required for formation of new adsorption sites. The "novelty" of these adsorption sites can probably be most adequately discussed in terms of the local modification of the work function of Ag. The effect of adsorbed chlorides on the work function of Ag has been discussed in several papers^{5,10,33} and interpreted as its local decrease. Nevertheless, the coincidence of the threshold chloride coverage for Ag-bpy surface species generation with that required for the onset of large morphological changes in Ag nanoparticle assembly suggests that the new adsorption sites could possibly originate also from the removal of oxidized Ag^+ (or Ag_n^+) adsorption sites and from the exposure of neutral Ag(0) adsorption sites in the course of the surface structure changes which, in turn, can be expected to accompany the observed Ag nanoparticle fusion. Two possible

mechanisms could be envisaged per analogiam with the results reported in studies of chloride-modified single crystal electrodes: either the dissolution of $[\text{AgCl}_2]^-$ complex ions, or the increased mobility of Ag^+ adatoms.^{34,35} Regardless of the actual mechanism of the new adsorption sites' formation, the work function of these adsorption sites is expected to be lower in comparison to that of the oxidized Ag^+ (or Ag_n^+), and the new adsorption sites could thus be considered as reduced. Consequently, we have proposed that such reduced adsorption sites should exist, and Ag-bpy surface species should be formed, in a strongly reducing ambient (in the absence of any surface-modifying ions as chlorides). Therefore, as a next step, we have probed the formation of bpy surface species in a system with Ag nanoparticles forming under strongly reducing conditions.

3.2 SERS spectral probing of systems prepared by chemical reduction-driven Ag nanoparticles growth in the presence of bpy and in the absence of chlorides

The SERS spectrum of bpy obtained from the system in which Ag nanoparticles were prepared in aqueous ambient by the reduction of silver nitrate by sodium borohydride in the presence of bpy molecules (further denoted bpy-Ag colloid system) at 514.5 nm (Fig. 7) matches that of Ag-bpy obtained by FA of spectra Ag colloid/bpy/HCl measured at the same wavelength (Fig. 2B), and indicates that the SERS spectra originate from the same surface species, *i.e.* Ag-bpy. The two SERS spectra (Fig. 7 and 2B) coincide not only in the wavenumbers of the spectral bands, but also in their relative intensities, as demonstrated *e.g.* by exactly the same value (3.0) of the relative band intensity ratio of the 1488/1602 cm^{-1} band. This ratio is highly sensitive to a change of the excitation wavelength in the SERS experiment, yielding a value of 2.1 in SERS spectra excited at 496 nm, and of 5.0 at 541 nm (spectral data from ref. 12 were used for comparison). Therefore, we argue that the relative intensity match indicates that the wavenumber position of the resonant photo-induced CT

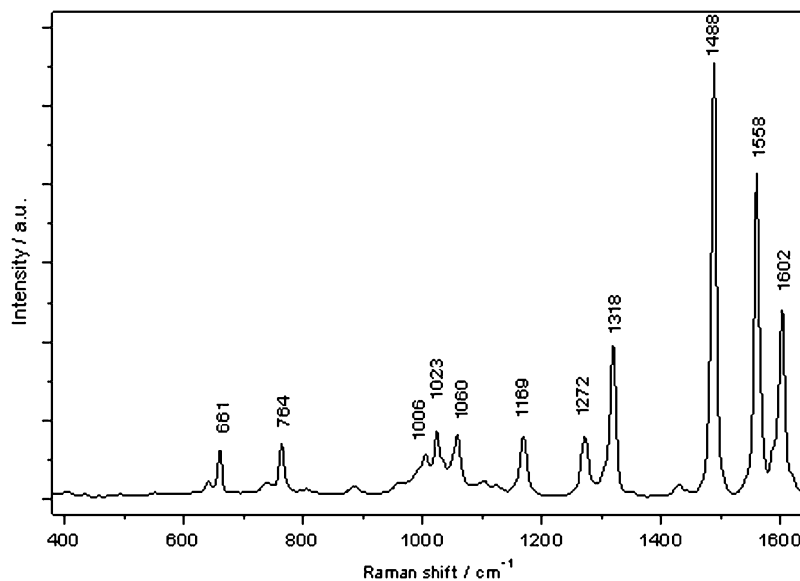


Fig. 7 SERS spectrum of Ag-bpy surface species prepared by reduction of AgNO_3 by NaBH_4 in the presence of 1×10^{-5} M bpy.

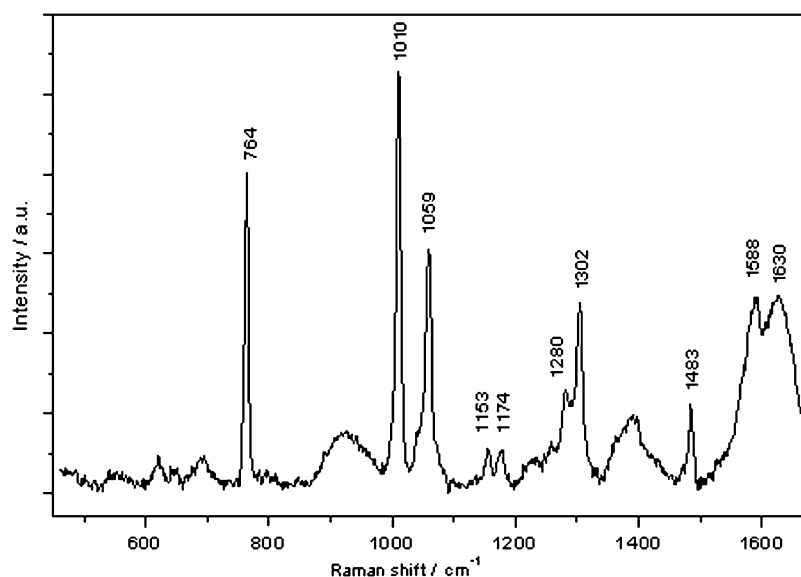


Fig. 8 SERS spectrum of the Ag^+ -bpy surface species generated in the Ag colloid/bpy system by 1×10^{-5} M bpy addition to the pre-prepared Ag colloid.

transition is virtually the same for the Ag-bpy species identified by FA in the system with the chloride-modified Ag nanoparticles and bpy, and for that detected in bpy-Ag colloid system. In the latter system, no chlorides or other strongly adsorbing ions were present, and the formation of the Ag-bpy species is attributed to the presence of neutral Ag adsorption sites in the strongly reducing ambient (with a redox potential of about -0.3 V, as reported in ref. 36 and 37).

We support our argument with the results of a reference experiment, in which bpy was added to Ag nanoparticle hydrosol pre-prepared by the same procedure of the reduction of silver nitrate by sodium borohydride, but in the absence of bpy. SERS spectrum obtained from this system (Fig. 8) matches that of Ag^+ -bpy obtained by FA (Fig. 2A) and, in accord with the previous studies,^{11,12,23} is attributed to bpy adsorbed on the oxidized Ag^+ or Ag_n^+ adsorption sites (*i.e.* those commonly available on routinely used, pre-prepared bh-red Ag colloids which were not subjected to any other chemical treatment and in which the redox potential is positive^{36,37}). Hence, we conclude that the new adsorption sites formed on Ag nanoparticle surfaces (in bh-red Ag nanoparticle hydrosols) at 0.6 and higher fractional chloride coverages are reduced Ag(0) adsorption sites. An interesting parallel to our results is represented by ref. 9, in which the formation of reduced Au(0) adsorption sites induced by adsorption of chlorides on Au nanoparticle surfaces is reported.

4. Conclusions

The treatment of Ag nanoparticles in bh-reduced hydrosols by chlorides in both acidic and neutral ambient results into the modification of nanoparticles by adsorbed chlorides. The adsorption of chlorides on the Ag nanoparticles is promoted in acidic ambient. In particular, the treatment of Ag nanoparticles by 5×10^{-3} M NaCl and HCl results into estimated 0.6 and 0.8–0.9 fractional coverages, respectively. The cov-

erages are related to Ag nanoparticles of 10 nm in size present in the fairly monodisperse, parent bh-red Ag colloid.

The effect of modification of Ag nanoparticles by adsorbed chlorides is distinctly different for low (<0.6) and high (>0.6) fractional chloride coverages. The threshold concentration of chlorides in solution required for the conversion of a system with low coverage (S1) into that with the high coverage (S2) is 5×10^{-4} M in acidic ambient (HCl) and 5×10^{-3} M in neutral ambient (NaCl).

In Ag colloid/ Cl^- /bpy systems with the low chloride coverages (S1), the adsorption of chlorides promotes the aggregation of parent Ag nanoparticles into fractal aggregates. The presence of oxidized Ag^+ or Ag_n^+ adsorption sites is witnessed by the SERS spectral detection of Ag^+ -bpy. The same adsorption sites were identified on the chemically untreated surfaces of parent Ag nanoparticles. The adsorption of chlorides at low coverages thus did not change the oxidized/reduced character of the available adsorption sites.

By contrast, in Ag colloid/ Cl^- /bpy systems with the high chloride coverages (S2), Ag-bpy surface species was identified. The geometric as well as the electronic structure of this surface species were found to be the same as that of the Ag-bpy surface species formed in a strongly reducing ambient of *ca.* -0.3 V under the conditions of Ag nanoparticle growth by the reduction of silver nitrate by sodium borohydride in the presence of bpy and in the absence of chlorides. The formation of the identical Ag-bpy surface species in both systems was attributed to the presence of reduced Ag(0) adsorption sites and their stabilization by adsorbed bpy. Reduced Ag(0) adsorption sites are seen to differ from the oxidized Ag^+ or Ag_n^+ adsorption sites (commonly available on the chemically untreated surfaces of the bh-red Ag nanoparticles) by a locally reduced work-function of Ag.

Furthermore, in the Ag colloid/ Cl^- /bpy systems with the high chloride coverages (S2), the formation of Ag-bpy surface species was found to be accompanied by dramatic changes in Ag nanoparticle morphology. The changes can be described as

the fusion of originally uniform (10 nm) Ag nanoparticles assembled in fractal aggregates into the compact aggregates of touching and/or interpenetrating (intergrown into twins, triples *etc.*) particles enlarged in the average sizes to 30–100 nm. The driving force of the morphology changes can most probably be attributed to the minimization of the surface energy of the system (in accord with explanations provided in other cases of observed nanoparticle fusion³⁸). In addition to that, the increase of the SERS-activating effect of chlorides was found to accompany conversion of S1 into S2, manifesting itself by a *ca.* 40× increase of the overall enhancement of SERS of bpy excited at 514.5 nm. The contribution of the chemical mechanism of SERS (stemming from the vicinity of the 514.5 nm excitation to the ~540 nm maximum of the photoinduced CT transition exhibited by the Ag-bpy surface species) was estimated to approximately one order of magnitude. The impact of new Ag nanoparticle morphologies encountered in S2 on the EM mechanism of SERS and on single molecule level SERS is fully revealed in ref. 32.

Finally, the pure component SERS spectra of Ag⁺-bpy and Ag-bpy are proposed to be employed for an unequivocal identification of each of the surface species. Bpy can thus serve as a probing adsorbate for the identification of Ag(0) adsorption sites *via* SERS spectral detection of the Ag-bpy surface species.

Acknowledgements

Financial support by 203/07/0717, grant awarded by Grant Agency of Czech Republic, and by MSM 0021620857, long-term research program awarded by MSMT of Czech Republic, is gratefully acknowledged.

References

- 1 M. Moskovits, *Rev. Mod. Phys.*, 1985, **57**, 783.
- 2 K. Kneipp, Y. Wang, H. Kneipp, L. T. Perelman, I. Itzkan, R. R. Dasari and M. S. Feld, *Phys. Rev. Lett.*, 1997, **78**, 1667.
- 3 A. M. Michaels, J. Jiang and L. Brus, *J. Am. Chem. Soc.*, 1999, **121**, 9932.
- 4 A. M. Michaels, J. Jiang and L. Brus, *J. Phys. Chem. B*, 2000, **104**, 11965.
- 5 A. Weiss and G. Haran, *J. Phys. Chem. B*, 2001, **105**, 12348.
- 6 W. E. Doering and S. Nie, *J. Phys. Chem. B*, 2002, **106**, 311.
- 7 M. Ishikawa, Y. Maruyama, J. Y. Ye and M. Futamata, *J. Lumin.*, 2002, **98**, 81.
- 8 P. Hildebrandt and M. Stockburger, *J. Phys. Chem.*, 1984, **88**, 5935.
- 9 D. A. Weitz, M. Y. Lin and C. Sandroff, *J. Surf. Sci.*, 1985, **158**, 147.
- 10 S. Schneider, H. Grau, P. Halbig, P. Freunshardt and U. Nickel, *J. Raman Spectrosc.*, 1996, **27**, 57.
- 11 M. Kim and K. Itoh, *J. Phys. Chem.*, 1987, **91**, 126.
- 12 I. Srnová, B. Vlčková, T. L. Snoeck, D. J. Stufkens and P. Matějka, *Inorg. Chem.*, 2000, **39**, 3551.
- 13 K. Kneipp, R. R. Dasari and Y. Wang, *Appl. Spectrosc.*, 1994, **48**, 951.
- 14 E. J. Liang, X. L. Ye and W. Kiefer, *J. Phys. Chem. A*, 1997, **101**, 7330.
- 15 S. Sanchez-Cortez, J. V. Garcia-Ramos, G. Morcillo and A. Tinti, *J. Colloid Interface Sci.*, 1995, **175**, 358.
- 16 B. Vlčková, P. Matějka, J. Šimonová, P. Pančoška, K. Čermáková and V. Baumruk, *J. Phys. Chem.*, 1993, **97**, 9719.
- 17 K. Solečká-Čermáková, B. Vlčková and F. Lednický, *J. Phys. Chem.*, 1996, **100**, 4954.
- 18 I. Šloufová-Srnová and B. Vlčková, *Nano Letters*, 2002, **2**, 121.
- 19 B. Schrader, *Infrared and Raman Spectroscopy (Methods and Applications)*, WCH, Weinheim, 1995, pp. 115–120.
- 20 E. R. Malinowski, *Factor Analysis in Chemistry*, Wiley, New York, 1991.
- 21 J. Hanzlíková, M. Procházka, J. Štěpánek, V. Baumruk, J. Bok and P. Anzenbacher, *J. Raman Spectrosc.*, 1998, **29**, 575.
- 22 J. Hanuš, K. Chmelová, J. Štěpánek, P. Y. Turpin, J. Bok, I. Rosenberg and Z. Točík, *J. Raman Spectrosc.*, 1999, **30**, 669.
- 23 I. Srnová, B. Vlčková, I. Němec, M. Šlouf and J. Štěpánek, *J. Mol. Struct.*, 1999, **483**, 213.
- 24 B. Vlčková, C. Douketis, M. Moskovits, V. M. Shalaev and V. A. Markel, *J. Chem. Phys.*, 1999, **110**, 8080.
- 25 D. Hecht and H. H. Strehblow, *J. Electroanal. Chem.*, 1997, **440**, 211.
- 26 The fractional coverage of Ag nanoparticles by adsorbed chlorides was calculated in the following manner: The amount of Ag was obtained from the amount of silver nitrate reduced during Ag nanoparticle hydrosol preparation. The average size of Ag nanoparticles (10 ± 2 nm) was determined by TEM image analysis and used for calculation of the amount and the surface area of Ag nanoparticles. Full coverage of the Ag nanoparticles by adsorbed chlorides was calculated using a simple overlayer model (T. Kramar, D. Vogtenhuber, R. Podloucky and A. Neckel, *Electrochim. Acta*, 1995, **40**, 43). Fractional coverages of Ag nanoparticles by chlorides were calculated using the amount of adsorbed chlorides determined from the Ag:Cl ratio established by EDX analysis.
- 27 F. J. Garcia-Vidal and J. B. Pendry, *Phys. Rev. Lett.*, 1996, **77**, 1163.
- 28 H. Xu, J. Aizpura, M. Kall and P. Apell, *Phys. Rev. E*, 2000, **62**, 4318.
- 29 S. Corni and J. Tomasi, *Chem. Phys. Lett.*, 2001, **342**, 135.
- 30 M. I. Stockman, V. M. Shalaev, M. Moskovits, R. Botet and T. F. George, *Phys. Rev. B*, 1992, **46**, 2821.
- 31 P. Zhang, T. L. Haslett, C. Douketis and M. Moskovits, *Phys. Rev. B*, 1998, **57**, 15513.
- 32 M. Sládková, B. Vlčková, P. Mojžeš, M. Šlouf, C. Naudin and G. Le Bourdon, *Faraday Discuss.*, 2006, **132**, 121.
- 33 D. H. Jeong, N. H. Jang, J. S. Suh and M. Moskovits, *J. Phys. Chem.*, 2000, **104**, 3594.
- 34 W. Kautek, S. Dieluweit and M. Sahre, *J. Phys. Chem. B*, 1997, **101**, 2709.
- 35 D. D. Sneddon, D. M. Sabel and A. A. Gewirth, *J. Electrochem. Soc.*, 1995, **142**, 3027.
- 36 D. L. Van Hynning, W. G. Klemperer and C. F. Zukoski, *Langmuir*, 2001, **17**, 3120.
- 37 D. L. Van Hynning, W. G. Klemperer and C. F. Zukoski, *Langmuir*, 2001, **17**, 3128.
- 38 E. Adachi, *Langmuir*, 2001, **17**, 3863.